Published in final edited form as:
Acta Neuropathol. 2011 May ; 121(5): 635–649. doi:10.1007/s00401-011-0798-y.

Granular expression of prolyl-peptidyl isomerase PIN1 is a constant and specific feature of Alzheimer's disease pathology and is independent of tau, Aβ and TDP-43 pathology

Ayoub Dakson,
Mental Health and Neurodegeneration Research Group, School of Community Based Medicine, Faculty of Medical and Human Sciences, Hope Hospital, Greater Manchester Neurosciences Centre, University of Manchester, Stott Lane, Salford M6 8HD, UK

Osamu Yokota,
Mental Health and Neurodegeneration Research Group, School of Community Based Medicine, Faculty of Medical and Human Sciences, Hope Hospital, Greater Manchester Neurosciences Centre, University of Manchester, Stott Lane, Salford M6 8HD, UK

Department of Neuropsychiatry, Okayama University Graduate School of Medicine, Dentistry and Pharmaceutical Sciences, 2-5-1 Shikata-cho, Okayama 700-8558, Japan

Margaret Esiri,
Neuropathology Department, Level 1 West Wing, John Radcliffe Infirmary, University of Oxford, Oxford OX3 9DU, UK

Eileen H. Bigio,
Department of Pathology, Northwestern University Feinberg School of Medicine, Chicago, IL 60619, USA

Michael Horan,
Mental Health and Neurodegeneration Research Group, School of Community Based Medicine, Faculty of Medical and Human Sciences, Hope Hospital, Greater Manchester Neurosciences Centre, University of Manchester, Stott Lane, Salford M6 8HD, UK

Neil Pendleton,
Mental Health and Neurodegeneration Research Group, School of Community Based Medicine, Faculty of Medical and Human Sciences, Hope Hospital, Greater Manchester Neurosciences Centre, University of Manchester, Stott Lane, Salford M6 8HD, UK

Anna Richardson,
Mental Health and Neurodegeneration Research Group, School of Community Based Medicine, Faculty of Medical and Human Sciences, Hope Hospital, Greater Manchester Neurosciences Centre, University of Manchester, Stott Lane, Salford M6 8HD, UK

David Neary,
Mental Health and Neurodegeneration Research Group, School of Community Based Medicine, Faculty of Medical and Human Sciences, Hope Hospital, Greater Manchester Neurosciences Centre, University of Manchester, Stott Lane, Salford M6 8HD, UK

Julie S. Snowden,

Correspondence to: David M. A. Mann, david.mann@man.ac.uk.

Mental Health and Neurodegeneration Research Group, School of Community Based Medicine, Faculty of Medical and Human Sciences, Hope Hospital, Greater Manchester Neurosciences Centre, University of Manchester, Stott Lane, Salford M6 8HD, UK

Andrew Robinson,
Mental Health and Neurodegeneration Research Group, School of Community Based Medicine, Faculty of Medical and Human Sciences, Hope Hospital, Greater Manchester Neurosciences Centre, University of Manchester, Stott Lane, Salford M6 8HD, UK

Yvonne S. Davidson, and
Mental Health and Neurodegeneration Research Group, School of Community Based Medicine, Faculty of Medical and Human Sciences, Hope Hospital, Greater Manchester Neurosciences Centre, University of Manchester, Stott Lane, Salford M6 8HD, UK

David M. A. Mann
Mental Health and Neurodegeneration Research Group, School of Community Based Medicine, Faculty of Medical and Human Sciences, Hope Hospital, Greater Manchester Neurosciences Centre, University of Manchester, Stott Lane, Salford M6 8HD, UK

David M. A. Mann: david.mann@man.ac.uk

Abstract

Alzheimer's disease (AD) manifests with progressive memory loss and decline of spatial awareness and motor skills. Neurofibrillary tangles (NFTs) represent one of the pathological hallmarks of AD. Previous studies suggest that the enzyme prolyl-peptidyl *cis–trans* isomerase PIN1 [protein interacting with NIMA (never in mitosis A)-1] recognizes hyperphosphorylated tau (in NFTs) and facilitates its dephosphorylation, thereby recovering its function. This study aims to determine the frequency, severity and distribution of PIN1 immunoreactivity and its relationship to NFTs and other neuropathological markers of neurodegeneration such as amyloid-β (Aβ) plaques and transcription-responsive DNA-binding protein of M_r 43 kDa (TDP-43). Immunohistochemical analysis of 194 patients (46 with AD, 43 with Parkinson's disease/dementia with Lewy bodies, 12 with progressive supranuclear palsy/corticobasal degeneration, 36 with frontotemporal lobar degeneration, 21 with motor neuron disease and 34 non-demented (ND) individuals) revealed an increased frequency and severity of PIN1 immunoreactive inclusions in AD as compared to all diagnostic groups ($P < 0.001$). The hippocampal and cortical distribution of PIN1 granules was distinct from that of NFTs, Aβ and TDP-43 pathologies, though the frequency of neurons with PIN1 immunoreactivity increased with increasing NFT pathology. There was a progressive increase in PIN1 changes in ND individuals as the degree of AD-type pathological changes increased. Present findings indicate that PIN1 changes are a constant feature of AD pathology and could serve as a biomarker of the onset or spread of AD neuropathology independent of tau or Aβ.

Keywords

Alzheimer's disease; PIN1; Neurofibrillary tangles; Neurodegeneration; Dementia

Introduction

Alzheimer's disease (AD) manifests as an impairment of memory with progressive loss of spatial awareness and ability to perform previously learnt motor skills. About 5% of people older than 65 years are diagnosed with AD [8], accounting for up to two-thirds of all cases of dementia [21, 42]. Dementia with Lewy bodies (DLB) and fronto-temporal lobar degeneration (FTLD) are also common causes of primary degenerative dementia. In FTLD,

the pathology is most often confined to the frontal and anterior temporal lobes bilaterally [13, 35, 37], and about 45% of cases show a pathological accumulation of tau proteins, in the form of Pick bodies or neurofibrillary tangles (NFTs) [43], the latter being immunohistochemically similar to those in AD. Therefore, much attention has been focused on investigating the distribution and mechanism of formation of NFTs, which are considered by many to precede the loss of nerve cells in these disorders.

The assembly of microtubules from tubulin is a prerequisite for the normal neuronal cytoskeleton, which in turn supports synaptic extensions and maintains cellular polarity and axonal transport of micromolecules and organelles. The microtubule-associated protein tau regulates the polymerization of tubulin and maintains microtubule stability in vitro [11]. The stability of microtubules is associated with normal tau binding affinity, which is regulated by reversible phosphorylation [40]. In AD, tau becomes abnormally hyperphosphorylated [6, 18] and forms insoluble filamentous aggregates termed paired helical filaments (PHFs) [1]. Hyperphosphorylation of tau reduces microtubule binding in vitro with loss of microtubule stability and buildup of NFTs [30]. Western blot analysis of AD brain shows an eightfold increase in phosphorylated tau, as compared to age-matched controls [24]. High levels of abnormal tau protein correlate with poor clinical outcome with the number of NFTs in cerebral cortex being associated with increasing cognitive impairment [3]. In addition, studies in transgenic mice bearing the substitution of proline for leucine at amino acid 301 (P301L) (the most common *MAPT* mutation in FTLD) showed motor and behavioural impairment with a gene dose-dependent progressive accumulation of phosphorylated tau in the form of PHFs [19, 26].

In 1999, Lu and colleagues [30] described a post-phosphorylation regulatory mechanism of tau phosphorylation mediated by the peptidyl-prolyl isomerase (PPIase) PIN1 [protein interacting with NIMA (never in mitosis A)-1]. PIN1 catalyses the isomerization of phosphorylated serine (Ser) and threonine (Thr) residues preceding proline (Pro) motifs (Ser/Thr-Pro) from *cis* to *trans* isomers [4]. It consists of two domains including an N-terminal WW domain, which binds substrates specifically at phosphorylated Ser/Thr-Pro motifs, and a C-terminal PPIase domain catalysing the cis/trans isomerization of these motifs to regulate protein function through conformational change [29]. This step has been shown to be crucial for the recognition of phosphorylated tau by conformational-specific phosphatases such as PP2A, which binds to the *trans* isomer of phosphorylated Ser/Thr-Pro [30].

In AD brain extracts, PIN1 has been shown to co-purify with PHFs [30]. An interaction between tau and PIN1 is thought to facilitate the dephosphorylation of hyperphosphorylated tau in vitro by PP2A, restoring the ability of tau to bind microtubules and promote microtubule stability. A deficiency of PIN1 expression has been postulated to impair tau dephosphorylation leading to aberrant tau hyperphosphorylation and formation of NFTs in hippocampal and cortical neurons.

In this study, we have determined the relative frequency, severity and distribution of PIN1 immunoreactivity in the brains of patients with AD and other neurodegenerative disorders, and in non-demented individuals. The aim was to determine the impact of PIN1 expression on the distribution and abundance of NFT pathology and whether the absence or presence of other pathological features of AD, such as amyloid-β (Aβ) plaques or transcription-responsive DNA-binding protein of M_r 43 kDa (TDP-43) inclusions, influenced these disorders.

Materials and methods

Cases

Formalin-fixed, paraffin-embedded sections (6 μm) of frontal and temporal cortex with hippocampus were available from 194 cases, with or without neurodegenerative disease, drawn from the Manchester Brain Bank. All tissues had been collected through appropriate consenting procedures with ethical approval. The study population consisted of 46 patients with AD, 43 patients with Lewy body disease (LBD) [34 patients with Parkinson's disease (PD) and 9 with DLB], 36 patients with FTLD, 9 patients with progressive supranuclear palsy (PSP), 3 patients with corticobasal degeneration (CBD) and 21 patients with motor neuron disease (MND). The FTLD group comprised 7 with FTLD-TDP type 1, 7 with FTLD-TDP type 2, 11 with FTLD-TDP type 3, 2 with FTLD-FUS, 4 with FTLD-tau with Pick bodies, 4 with FTLD with *MAPT* gene mutations (3 with N297K, 1 with exon 10 + 16 mutation) and 1 with FTLD-ni (no inclusions) (classification according to recent consensus criteria [32, 33]).

In addition, 34 non-demented (ND) cases comprising 31 cases without any history of cognitive or psychiatric disorders prior to death and 3 cases with mild cognitive impairment (MCI) were investigated. The ND group included seven cases with no evidence of NFT and Aβ plaque pathologies. Of these 34 cases, 12 were obtained from Thomas Willis Brain Bank, Department of Neuropathology, University of Oxford. Again, these had been collected through appropriate consenting procedures with ethical approval. Selected demographic details are provided in Table 1.

Postmortem delay times were widely variable, though usually removal of the brain and its placement into formalin fixative was accomplished within 24–48 h.

Immunohistochemistry

Paraffin sections cut at 6 μm thickness were immunostained for PIN1 using three commercially available goat polyclonal antibodies (A-20 and C-20 (sc-7409), Santa Cruz Biotechnology Inc., Santa Cruz, CA, USA and SAB2500793, Sigma–Aldrich, Poole, Dorset, UK), all at a dilution of 1:200. All three antibodies are affinity purified and detect a single band of ~ 17 kDa corresponding to MW of PIN1. The Santa Cruz antibodies have been extensively used and validated by others [19, 23, 39]. A standard immunostaining procedure was followed [12, 13]. Briefly, all sections underwent antigen retrieval with microwave heating at 0.1 M citrate buffer, pH 6.0, for 10 min. In order to quench endogenous peroxidase activity, slides were incubated in 0.3% peroxide in methanol for 30 min. Using VECTASTAIN ABC kit (Vector Laboratories, Peterborough, UK), sections were incubated for 1 h or overnight (at 4°C) in blocking buffer to mask non-specific binding sites, followed by 1-h immunostaining with anti-PIN1 antibody. Following 5-min PBS washes, incubation in biotinylated secondary antibody and avidin–biotin complex were performed for 30 min each. The reaction was visualized using 3,3′-diaminobenzidine (DAB) (Sigma, Poole, Dorset, UK). Sections were lightly counterstained with haematoxylin and dehydrated sequentially through a series of alcohol and xylene solutions.

Adjacent sections of frontal and temporal cortex from all 194 cases were immunostained for tau [using AT8 antibody (Innogenetics, Antwerp, Belgium 1:750)], Aβ [using 4G8 antibody (Covance Research Products Inc., Dedham, MA, USA, 1:3000)] and TDP-43 (using either a phospho-independent (AP10782-2-AP, Proteintech, Manchester, UK, 1:1000) or a phospho-dependent [pS409/410-2 antibody (Cosmo Bio Co., Ltd, Tokyo, Japan, 1:3000) antibody]. Double labelling immunofluorescence was not performed (see "Discussion").

Pathological assessment

The severity of PIN1-positive inclusions affecting the pyramidal neurons of CA regions of hippocampus, subiculum, entorhinal cortex, frontal and temporal neocortex and granular neurons of dentate gyrus was graded semi-quantitatively on a five-point scale. The scoring system required counting the number of PIN1-positive neurons at 200× magnification in each anatomical region using the following definitions for each stage;

0 = absent

1 = mild (1 positive neuron/1 field at least)

2 = moderate (>1 positive neuron/2 fields at least)

3 = severe (≥4 positive neurons/2 fields at least)

4 = very severe (>10 positive neurons/2 fields at least)

Neurons were counted as positive irrespective of the actual number of PIN immunoreactive granules present, or whether the PIN1 granules were diffusely and apparently freely present throughout the neuron or whether they were associated with a surrounding vacuole in the form of GVD.

The same scoring system was used to assess the frequency of NFT pathology for the purpose of direct comparison with the frequency of PIN1 immunoreactivity. Ten anatomical subregions of the hippocampal formation (as defined by Price et al. [39]) were graded, including CA4/5, CA3, CA2, CA1, subiculum/presubiculum and entorhinal cortex, and also within the fusiform gyrus, inferior and middle temporal gyri, mid frontal gyrus and primary visual and visual association (occipital) cortex (layer II) (where available). The overall severity score per case for PIN1 or NFTs (0–40) was obtained by summing all subregional scores. Results are expressed as means of overall severity scores per cases ±standard deviation (SD) for each group. The high number of samples and the many immunostains used in the present study made it impractical to employ a stereological methodology to assess the frequency of affected neurons.

The Braak staging system [9] for assessment of NFT pathology was applied to the AD, PD/DLB and ND groups.

Statistical analysis

All data analysis was performed using SPSS v 16.0. Differences of proportions of cases with PIN1 changes and its association with AD neuropathology across different diagnostic categories were assessed with Pearson chi-square test. To determine which proportion of diagnostic cases accounts for a significant result, post hoc analysis with a critical value of ±1.93 was applied. Kolmogorov–Smirnov (for $n > 50$) or Shapiro–Wilk (for $n < 50$) tests were used to determine whether data were normally distributed. For normally distributed data, two-sample Student's t test for independent samples or one-way ANOVA were applied in comparing means of PIN1 overall severity scores per cases between two or more groups, respectively. Alternatively, for non-normally distributed data, Kruskal–Wallis analysis of variance with post hoc Mann–Whitney U test was used. Similarly, when testing the correlations between overall severity scores and age at death, Spearman's first rank correlation or Pearson's correlation tests were used as appropriate. All levels of significance were two tailed and set at $P < 0.05$.

Results

The frequency and severity of PIN1 immunoreactive granules in AD compared to other diagnostic groups

PIN1 immunoreactivity occurred in hippocampal and/or cortical pyramidal neurons, but particularly in those of areas CA2/3 and CA1 of the hippocampus. As described previously by Holzer et al. [23] and Ramakrishnan et al. [40], PIN1 immunoreactivity was mostly seen as well-defined, spherical, punctuate and densely staining cytoplasmic granules, evenly distributed throughout the cell soma, and irrespective of cell type in which they occurred. On other occasions, the granules occurred within well-defined vacuoles, resembling the pathological change known as granulovacuolar degeneration (GVD) (Fig. 1a). When present, the granules bore the same morphological appearance and intracellular distribution in all diagnostic groups (Figs. 1, 2). There were no obvious differences in either staining intensity or intracellular distribution of PIN1 immunoreactive granules in any of the 3 PIN1 antibodies (not shown); however, because the C-20 antibody showed no background staining, it was decided to use this antibody for all subsequent work. The PIN1 granular staining was easily distinguished from any pale, hazy yellow, nonspecific staining of lipofuscin.

PIN1 immunoreactivity occurred in hippocampal pyramidal neurons and/or cortical neurons in 72.2% (n = 140) of all cases. All AD cases (48/48, 100%) contained hippocampal and/or cortical neuronal PIN1 granules as compared to fewer PD/DLB (34/43, 79.1%), FTLD (16/36, 44.4%), PSP/CBD (8/12, 66.7%), MND (66.7%) and ND (20/34, 58.8%) cases (Table 2). Chi-square analysis showed a statistically highly significant difference in the proportion of PIN1-positive cases between the different diagnostic groups ($\chi^2 = 3.68$, $P < 0.001$). Post hoc analysis revealed that more AD cases, and fewer FTLD cases, with PIN1 granules than expected were responsible for this significant difference.

Furthermore, we determined PIN1 overall severity scores in all diagnostic groups (Fig. 3). By Kruskal–Wallis analysis of variance, there was a highly significant difference in PIN1 overall severity scores between groups ($H = 94.9$, $P < 0.001$). Post hoc Mann–Whitney U comparison between pairs of groups showed that AD cases were affected more severely than PD/DLB, FTLD, PSP/CBD, MND and ND groups (post hoc Mann–Whitney U test, 11.4 ± 4.0 [AD] vs. 2.2 ± 2.0 [PD/DLB], 1.4 ± 2.3 [FTLD], 2.8 ± 2.5 [PSP/CBD], 2.4 ± 2.4 [MND] or 4.0 ± 4.5 [ND], all $P \leq 0.001$). The mean PIN1 overall severity score in the ND group was significantly higher than that of the FTLD ($P < 0.001$), but not significantly different from that in PD/DLB, PSP/CBD and MND ($P > 0.05$). Although the PD/DLB group had a significantly higher mean PIN1 overall severity score than the FLTD group ($P = 0.021$), there was no significant difference between PD/DLB, PSP/CBD ($P = 0.521$) and MND groups ($P = 0.942$). In addition, there was no significant difference between FTLD, MND and CBD/PSP groups ($P = 0.07$). According to this analysis, the following ranking orders of PIN1 severity could be obtained;

AD > PD/DLB, FTLD, PSP/CBD, MND and ND groups

ND and PD/DLB > FTLD

FLTD = MND = PSP/CBD

There were no significant differences in PIN1 severity scores between the different FTLD histological subtypes (Fig. 4).

The presence of PIN1 granules is independent of age at death

There was a significant difference in mean age at death between the disease groups (H = 30.3, $P < 0.001$). Although there were no significant differences in the age at death between PIN1-positive and PIN1-negative cases within AD, PD/DLB and FLTD groups ($P > 0.05$), PSP/CBD and ND cases with PIN1 immunoreactivity were significantly older than the PIN1-negative cases ($P = 0.016$ and $P = 0.003$, respectively) (Table 3). There were no significant correlations between age at death and PIN1 overall severity scores for all diagnostic groups ($P > 0.05$), except for the PSP/CBD ($P = 0.002$) and ND groups ($P < 0.001$). The difference in PIN1 overall severity scores among diagnostic groups cannot be explained by the differences in age at death alone, because although there was no significant difference in age between the AD and ND groups ($P = 0.162$), mean PIN1 overall severity score was significantly higher in AD cases as compared to ND cases ($P < 0.001$). By contrast, patients with PD/DLB were significantly older than patients with AD ($P = 0.008$) in whom PIN1 overall severity scores were higher than those in the PD/DLB cases, suggesting that high PIN1 severity is not related per se to increasing age in these groups. In addition, whereas the PSP/CBD group was significantly older than the FTLD group ($P = 0.009$), there was no significant difference in PIN1 severity scores between the PSP/CBD and FTLD groups.

The topographic distribution of PIN1 granules

The distribution of PIN1 granules followed a specific topographic pattern in all groups. In AD, hippocampal regions of CA1, CA2 and the subiculum were most frequently involved with up to 98% of AD cases having PIN1 granules in these regions (Fig. 5a). The frequency of PIN1 granules was very severe in CA1 in about 10% of cases, severe in 36%, moderate in 26% and mild in 24%, but absent in 4.0% of AD cases. Only 2.0% of AD cases had no PIN1 granules in CA2 subfield, with 46% of cases having severe involvement and 2.0% having very severe involvement. The subiculum was involved in 87% of AD cases with parallel severity scores. Involvement of the dentate gyrus (DG), CA4 and CA3 subfields occurred in 72–92% of AD cases, with the majority of these cases having mild severity scores. In contrast to hippocampal subareas, cortical regions either lacked PIN1 granules in 34–68% of AD cases or had minimal involvement, with the entorhinal cortex being most severely involved.

A similar distribution pattern of neuronal PIN1 granules occurred in the PD/DLB, PSP/CBD, FTLD and MND cases, but with a lower frequency (Figs. 5b, 6). The majority of cases had only a mild involvement by PIN1 granules, with fewer cases (than in AD) having severe or moderate involvement, and no cases with very severe involvement, except for the ND group (see below). In PD/DLB cases, CA2, CA1 and the subiculum were most severely involved in up to two-thirds of cases, as compared to less severe involvement of the DG, CA3 and CA4 subfields in less than quarter of the cases (Fig. 5b). PIN1 granules were absent in the temporal cortex and fusiform gyrus and could be detected in only 2.0% of cases in the entorhinal cortex. Similarly, more PSP/CBD cases had higher severity scores in CA2, CA1 and subiculum (Fig. 6b), as compared to the DG, CA4 and CA3 subfields. Whereas PD/DLB cases had almost no cortical involvement, up to 18% of PSP/CBD cases had PIN1 granules in the fusiform gyrus and entorhinal and temporal cortices.

While the distribution of PIN1 granules mirrored that in the PSP/CBD cases with somewhat similar severity scores (Fig. 6c), the FTLD cases, in contrast to all other diagnostic groups, had only very mild severity scores of PIN1 granules across all regions with no apparent preferential distribution (Fig. 6a).

The subregional severity scores of PIN1 granules in the ND cases were intermediate between AD and all other disease groups (Fig. 6d). CA1 and the subiculum had higher severity scores in the majority of cases. In contrast to AD, a greater cortical involvement was observed in the ND cases, whereas fewer cases had PIN1 granules in the DG, CA4 and CA3 subfields.

The topographic relationship between of PIN1 granules and NFTs

To ascertain the topographic relationship between the distribution patterns of PIN1 granules and NFTs, adjacent sections from 12 AD and 43 PD/DLB cases were separately stained for PIN1 and tau (NFTs) (Fig. 5). The topographic distribution of PIN1 granules across the different subfields of the hippocampus and adjoining neocortical regions demonstrated no consistent inverse or direct association with the distribution of NFTs. For instance, PIN1 granules occurred most severely in CA2 and CA1 regions and less severely or absent in the DG and cortical areas, whereas NFTs occurred most severely in CA1 subfield and in cortical areas, but less severely in the CA2 region (Fig. 5a).

In the 34 PD and 9 DLB cases, there was also no clear association between the distribution of NFTs and PIN1 granules (Fig. 5b). When present, NFTs occurred in CA1 subfield, the subiculum and entorhinal cortex with highest severity scores. This pattern shows no obvious inverse or direct subregional relationship with PIN1 granules affecting CA2, CA1 and the subiculum most severely, and NFTs occurring most severely in CA1 and subiculum, but not in the CA2 subfield. In addition, NFT-rich entorhinal and temporal cortices were nearly always lacking in PIN1 granules.

To test whether the overall severity score of PIN1 granules was related to that of NFTs, correlation tests in 12 AD, 43 PD/DLB and 12 MND cases were performed (Table 4). There was no significant relationship between the degree of severity of the two proteinopathies, except for a marginally significant association in the MND group ($P = 0.044$).

The relationship between PIN1 granules and AD-type pathological changes

Based on the Braak staging system on the distribution of NFT pathology [9], ND cases were subdivided into four groups including cases with Braak stage 0 ($n = 7$), stage I–II ($n = 14$), stage III–IV ($n = 13$) and stage V–VI ($n = 2$) (Fig. 7). The mean PIN1 overall severity score was significantly different across groups ($P < 0.001$). PIN1 mean overall severity score in ND cases with Braak stage 0 was significantly lower than cases with advanced Braak stages including stages III–IV ($P = 0.017$) and V–VI ($P < 0.001$), but not stage I–II ($P = 0.154$). There was no significant difference between cases with stage III–IV and V–VI ($P = 0.058$), but both groups of cases with stages III–IV and V–VI had higher scores than less advanced cases with stage I–II ($P < 0.001$ and $P = 0.017$, respectively). In this study, all AD cases had advanced Braak stages V–VI, which have a mean PIN1 overall severity score significantly higher than ND cases with Braak stage 0 ($P < 0.001$), I–II ($P < 0.001$) and III–IV ($P = 0.003$), but not different from ND cases with stage V–VI ($P = 0.727$) (Fig. 7). Therefore, the ranking order for PIN1 severity based on the degree of spread of NFTs pathology across different brain regions is: AD > ND (III–IV) > ND (I–II).

In PD/DLB, although those cases with higher Braak stages [9] did show numerically higher PIN1 severity scores, overall there were no significant differences in PIN1 severity scores between cases with different Braak stages ($P = 0.427$) (Fig. 8). There were insufficient FTLD and MND cases with Braak stages greater than zero for meaningful statistical analysis of PIN1 severity scores.

Tissue sections from 36 PD/DLB cases, 36 FTLD cases, 12 PSP/CBD cases and 29 ND cases were stained for Aβ plaques and PIN1 granules separately (Table 5). There were no

significant differences in the mean PIN1 overall severity scores between Aβ-positive and Aβ-negative cases in any of the diagnostic groups ($P > 0.1$), except for the ND group ($P = 0.006$).

Finally, we asked whether the severity of PIN1 changes across all diagnostic groups apart from AD was associated with the presence of Alzheimer's disease pathology, a positive case in this respect being defined as one with positive NFTs or/and β-amyloid plaques. By this analysis, the severity of PIN1 pathological changes in these other diagnostic groups was significantly related to the presence of AD pathological changes ($\chi^2 = 6.5$, $P < 0.001$). Post hoc analysis attributes this statistical significance to a higher (than expected) proportion of PD/DLB cases with PIN1 and AD-type changes. In addition, there was a significantly greater (than expected) proportion of FTLD cases without PIN1 and AD-type change (and therefore significantly fewer cases of FTLD with both PIN1 and AD-type changes), and a greater proportion of FTLD cases with PIN1 changes alone.

These data therefore only partially support the hypothesis that PIN1 is exclusively associated with AD-like change in other diagnostic groups.

The relationship between PIN1 granules and TDP-43 pathology in AD

A total of 32 AD cases were stained for TDP-43 pathology and PIN1 granules separately. The severity of PIN1 granules was unrelated to the presence or absence of TDP-43 pathology [11.6 ± 4.9 (TDP-43-positive) versus 11.3 ± 3.7 (TDP-43-negative), $P = 0.838$]. Moreover, the topographical distribution of PIN1 and TDP-43 pathological changes were almost mutually exclusive with TDP-43 changes being encountered in DG, entorhinal cortex, fusiform gyrus and temporal neocortex with only rare TDP-43 positive neurons being seen within the CA regions and subiculum (Fig. 9) (see above for topographic distribution of PIN1 changes).

Discussion

This is the first study comparing the degree of expression of the peptidyl-prolyl *cis–trans* isomerase PIN1 in hippocampal and cortical neurons in brains of patients with AD, other neurodegenerative disorders and ND cases. A large proportion of total study cases (75.0%) stained positive for PIN1 granules with FTLD and MND cases showing significantly fewer PIN1 granules, both in terms of the proportion of cases affected and the severity of involvement in individual cases. Visualization of PIN1 immunoreactive changes was consistent with previous reports describing well-defined, dark, punctate granules occasionally found within vacuoles of the cytoplasm of pyramidal and granular neurons, resembling GVD in such instances [23, 40]. GVD is characterized morphologically by the presence of discrete 0.5–5 μm basophilic granules, each within a clear vacuole, in the perikaryal cytoplasm of pyramidal neurons [34]. The granules contain an electrondense core surrounded by a translucent matrix on ultrastructural analysis [22]. The dense core has been shown to contain epitopes for a wide range of proteins including neurofilament protein, phosphorylated-tau, ubiquitin [15] and the mitosis-specific phospho-specific MPM-2 [45]. Indeed, Holzer et al. [23] noted that the majority of PIN1 granules were immunoreactive with an antibody to MPM-2. It is therefore possible that the high concentrations of PIN1 in GVD are due to PIN1 sequestration by phosphorylated proteins in GVD, given that PIN1 binds to many MPM-2 antigens.

Lipofuscin is a pale, naturally yellow–brown pigment universally accumulating in ageing post-mitotic cells including neurons, and is diffusely present in the cytoplasm of many neurons in tauopathies and non-tauopathies. Although in the present study (see results section) and that by Holzer et al. [23], the robust dark C-20 immunostaining of PIN1

granules was clearly differentiated from the pale yellow–brown lipofuscin ‘staining’, other investigators have regarded this latter pale staining as representing PIN1 immunostaining—an interpretation that might lead to the false-positive characterization of PIN1 granules [28, 40]. This similar, ill-defined ‘staining’ was observed with a different commercial anti-PIN1 antibody (A-20) [40] suggesting that such ill-defined inclusions might represent an early stage of PIN1 granular aggregation, or support an association between PIN1 granules and lipofuscin granules. The latter argument is supported by an immunogold-labelling study showing co-localization of PIN1 granules within lipofuscin granules in an ageing brain [19]. These authors speculated that PIN1 binding to lipofuscin might contribute towards a depletion of soluble PIN1 neuronal reserves. However, there are no studies that tested this hypothesis in AD.

Although an invariable accompaniment to AD [5, 44], GVD is generally excluded from case assessments using standardized pathological criteria for diagnosis of AD, due to its frequent presence as an ‘incidental finding’ in controls—a property that coincidentally is shared with both senile plaques and NFTs.

PIN1 granules occurred in a large proportion of cases across all groups within the hippocampal regions of CA2, CA1, subiculum and presubiculum, with minimal occurrence or complete absence in the entorhinal and temporal cortices. Involvement of other hippocampal regions such as the dentate gyrus, CA4 and CA3 was variable in the different groups, being intermediate between cortical areas having scarce PIN1 granules and regions of CA2, CA1 and subiculum having a more severe involvement. These observations lead to the question as to whether PIN1 pathology is indeed GVD with the scattered intracellular distribution of small, apparently non-membrane bound granules representing a ‘pathological forerunner’ of the larger obviously membrane-bound granules residing within vacuoles, the latter being perhaps derived from a gradual fusion and coalescence of the smaller individual granules into the vacuolated structure.

The pathogenic significance of GVD has been addressed only superficially, and are considered ‘autophagic lysosomal structures’ (autophagic vacuoles) in which cytoskeletal and many other proteins are degraded [14]. Present observations accord with such a viewpoint. Interestingly, it has recently been reported [10] that GVD contain phosphorylated-S6 protein, a marker of stress granules, suggesting a relationship between this and oxidative damage or changes in RNA metabolism, leading to neurodegeneration in AD. Furthermore, early studies noted the presence of GVD within hippocampal neurons in Pick’s disease [22], and the present findings of PIN1 pathology, but of less severe degree than usually associated with AD, in cases of FTLD-tau and FTLD-TDP would accord with such observations.

Although the distribution of PIN1 granules was largely uniform across different brains despite the presence of different co-existing pathologies such as NFTs, Aβ plaques and TDP-43 inclusions, PIN1 granules were observed in all AD cases with a much higher severity score compared to all other groups ranging between 8.2- and 1.7-fold greater than in FTLD cases (with lowest PIN1 severity) and ND cases (with highest PIN1 severity after AD), respectively. These results imply that AD represents the main scenario for PIN1 granules, showing a similar topographic distribution in all other groups (except FTLD) to that seen in AD, but at a lower frequency and severity.

PIN1 has been shown to co-purify with phosphorylated tau in the form of PHFs extracted from AD brains as compared to the absence of PIN1 in PHFs from age-matched normal brains [30]. Up to date, a number of reports have been published to evaluate the association between PIN1 and NFTs in vivo. Holzer et al. [23] performed double labelling

immunofluorescence on hippocampal tissue sections from AD cases using four different antisera directed against PIN1, including two commercially available goat anti-PIN1 antibodies (C-20 and N-19, both 1 in 50) and two synthetic rabbit anti-PIN1 antibodies (PinA and PinB, both 1 in 2000). A range of different antibodies recognizing tau was used to test PIN1 co-localization to phosphorylated (AT8, AT180, AT270, PHF1 antibodies) and unphosphorylated tau (BR134, BR 135, BR189, Tau-2 and HT7 antibodies) epitopes. Although PIN1 immunoreactive granules were stained intensely in the cytoplasm of CA1 and CA2 regions, no co-localization could be detected between PIN1 granules and tau aggregates. In addition, Ramakrishnan and colleagues [40] tested co-localization of NFTs and PIN1 in AD and other tau-rich disorders (tauopathies) including FTLD and PSP. The authors used two different goat anti-PIN1 antibodies (C-20 and A-20, 1:200) and one mouse anti-phosphorylated-tau antibody (TG3, 1:25) but likewise could not detect co-localization between neurofibrillary lesions and PIN1 granules. On the other hand, both studies [22, 40] detected a very occasional co-localization between PIN1 and phosphorylated tau when representing pre-tangles, rather than classic tangles, of AD.

In this study, we examined the relationship between the frequency and distribution of PIN1 and NFTs in different diagnostic groups. The subregional distribution of PIN1 granules in the hippocampus and cortical areas was independent of that of NFT pathology in AD and PD/DLB. Furthermore, bivariate correlation test failed to detect any significant association between the overall severity scores of PIN1 and NFTs in three separate disease groups including AD, PD/DLB and MND, suggesting that the frequency of NFT pathology was independent of that of PIN1 granules. Interestingly, the PIN1 severity score was greater in the ND cases with advanced Braak stages III–IV and V–VI as compared to Braak stage I–II. In other words, while the degree of PIN1 severity in advanced tauopathy in AD and ND cases with Braak stage V–VI tends to be higher, cases where the tauopathy is limited to the transentorhinal and entorhinal regions, CA1 and CA2 hippocampal subfields (Braak stage I–II) are more likely to have a lower PIN1 severity score, as compared to cases where NFT pathology has spread more widely into the fusiform and neocortical association areas (Braak stages III–IV) and primary and secondary neocortical areas of the occipital and frontal lobes (Braak stages V–VI). These findings are in agreement with a previous study reporting the absence or a very low frequency of PIN1 granules in five normal brains with NFT pathology limited to the entorhinal cortex only [38]. In addition, Holzer et al. [23] described a very low frequency of PIN1 granules in the subiculum, CA1, CA2 and CA3 subfields in five normal controls; however, the authors described their control cases as having ‘no pathological signs’ without clearly defining the presence of any NFT pathology. Nonetheless, the very low severity of PIN1 granules in ND brains with NFT pathology restricted to the entorhinal and CA1/2 regions or complete absence of PIN1 granules in ND cases free of any NFT pathology suggests that increased frequency of PIN1 granules requires, or at least associates with, an advanced and a widely spread tauopathy. This dichotomy between the distribution and spread of PIN1 and tau changes in AD and ND cases raises the question as to the role PIN1 changes play in the pathogenesis of AD, when according to Braak staging [9] the entorhinal cortex is the earliest site of tau involvement, and the temporal neocortex that of Aβ plaque deposition. Such observations further the argument that PIN1 pathological changes develop independently of tau and Aβ plaques, but their role in triggering or progressing the course of AD remains unclear.

Western blot analysis of whole brain homogenates has demonstrated a reduction of the soluble form of PIN1 as compared to an increased detection of its insoluble form in AD brain [27]. Because PIN1 binds phosphorylated tau (p-tau) in vitro, it has been hypothesized that aggregated tau might sequester and trap soluble PIN1 depleting its neuronal reserves (for reviews, see Refs. [4, 23]). Lack of evidence of co-localization of PIN1 granules to NFTs in AD as described by previous studies (see above) and absence of a direct

relationship between the severity of PIN1 granules and NFTs, with lack of overlapping distribution patterns of the two proteinopathies, do not support this viewpoint. Furthermore, Lu et al. [30] showed that addition of non-mutated PIN1 to a mixture of monomers of tubulin and p-tau increased the rate of tubulin polymerization and its assembly into microtubules, as compared to tubulin alone or tubulin with mutated PIN1. In addition, mice with PIN1 knockout develop age-dependent motor deficits, with accumulation of neuronal p-tau aggregates in the hippocampus in 66.6% of $PIN1^{-/-}$ mice [28]. Therefore, these authors suggested that an increased expression of PIN1 could be inversely associated with NFTs. Although the present study consistently shows an absence or a minimal frequency of neuronal PIN1 granules in cortical areas where NFT pathology is prominent, such a relationship dissociates in the hippocampal subfields of CA1 and subiculum where PIN1 granules and NFT pathology are equally prominent. The lack of direct evidence of co-localization, and of any significant association between the frequency and subregional distribution patterns of PIN1 and NFTs, does not support the notion of a major ‘de-tangling’ role of PIN1. However, such a hypothesis could be appropriately examined by testing whether the overexpression of PIN1 reduces NFTs in a cell culture or animal model of tauopathies.

The transcription-responsive DNA-binding protein of M_r 43 kDa (TDP-43), which is a nuclear protein involved in transcriptional repression and alternative splicing, forms a major pathological component of ubiquitin-positive and tau-negative inclusions in FTLD with ubiquitin inclusions and in amyotrophic lateral sclerosis [2, 36]. TDP-43 inclusions also occur in AD, affecting 34.4% of AD cases in this study. The presence or absence of TDP-43 pathology had no impact on the frequency of PIN1 granules. Furthermore, in PD/DLB and PSP/CBD cases, the presence or absence of Aβ plaques, which constitute a prominent extracellular pathological hallmark in AD, also had no impact on the frequency of PIN1 granules. Together, these findings indicate that the incidence of PIN1 granules represents a universal feature of AD that is independent of the frequency and distribution of NFT pathology, presence or absence of Aβ and TDP-43 pathologies, with PIN1 frequency increasing in more advanced NFT pathology.

In addition, we have reported for the first time PIN1 cytoplasmic inclusions in MND cases. MND is a progressive fatal neurodegenerative disease, which manifests clinically as progressive weakness, muscle wasting and spasticity resulting from selective loss of upper and lower motor neurons [38]. Two types of ubiquitinated aggregates have been reported in MND containing superoxide dismutase (SOD1) or TDP-43 [2]. Whether PIN1 granules play any role in MND pathogenesis through an interaction with NFTs, SOD1 or TDP-43 inclusions remains to be investigated.

Although we observed a positive relationship between age at death and absence/presence of PIN1 immunoreactivity or degree of PIN1 severity in ND cases, this can be explained by the fact that younger ND brains, which lack evidence of disease-like pathology such as NFTs and Aβ plaques, are also more likely to be free of PIN1 immunoreactive granules. Similarly, CBD/PSP cases with PIN1 immunoreactivity were significantly older than the PIN1-negative cases. It is presumed therefore that, as with normal people, those with neurodegenerative diseases other than AD, such as PSP/CBD, as they get older, become more likely to suffer/become susceptible to those processes that result in AD-associated pathologies as plaques and tangles, and consequently PIN1 changes likewise.

The principal clinical implication of this present study directs that PIN1 could serve as a potential biological marker of AD in plasma or cerebrospinal fluid, possibly distinguishing it from other neurodegenerative dementias, particular those in which phosphorylated tau is accumulated in the brain, as suggested by the highest frequency and severity of PIN1

granules in AD as compared to other disease groups. We have shown that in younger brains with no evidence of NFT pathology or Aβ plaques, there is no PIN1 immunoreactivity or very mild PIN1 severity. Together, these findings and the increased severity of PIN1 granules in ND cases with higher Braak stages suggest that PIN1 might serve as an early marker of Alzheimer-like pathology or could be useful in monitoring the development or progression of disease.

Current leading cerebrospinal fluid (CSF) biomarkers for AD are amyloid-β peptide with 42 amino acid mutation (Aβ1-42) [16, 17], total tau and tau phosphorylated at Thr 181 (p-tau181) [7, 45, 47]. The CSF ratio of p-tau181p/Aβ1-42 has been found to predict longitudinal cognitive decline in 84 individuals with mild cognitive impairment (MCI) [25]. Combined analysis of t-tau and Aβ1-42 improves diagnostic accuracy with 86% sensitivity and 97% specificity [31]. It can be postulated that PIN1 levels in the CSF, or plasma, might correlate with the presence or severity of its expression in the brain and could serve as a biomarker independent of tau or Aβ.

In summary, the enzyme prolyl-peptidyl isomerase PIN1 has been implicated in the pathogenesis of AD by interacting with tau inclusions. The role of PIN1 as a neuroprotective agent ameliorating NFT pathology requires further investigation. Its granular expression represents a constant feature of AD, with severity and distributional patterns independent of tau, Aβ and TDP-43 pathologies. It is suggested that changes in PIN1 evidence and parallel the onset and progression of Alzheimer's disease process, and may have potential utility as a biomarker if PIN1 can be detected in CSF or plasma. This could aid in early identification of ongoing AD-type pathology in individuals with suspected cognitive impairment, and distinguish AD from other neurodegenerative dementias. Future research will investigate whether PIN1 can indeed be detected in CSF, or even plasma, and whether levels of PIN1 correlate with AD neuropathology, or with disease progression and cognitive function.

Acknowledgments

We wish to thank the Academic Cultural Office of Kuwait, London, and the Ministry of Higher Education, Kuwait, who kindly provided grant support for this work. We thank The UK Parkinson's Disease Society Tissue Bank, the Thomas Willis Brain Bank, Oxford and Dr Eileen H Bigio (Northwestern Alzheimer Disease Center, AG13854, Northwestern University, Chicago, USA) who kindly provided some of the tissue samples employed in this study. We acknowledge the Alzheimer's Research Trust and Alzheimer's Society through the Brains for Dementia Research Initiative for supporting the work of the Manchester and Oxford Brain Banks. MME received financial support from the National Institute for Health Research (NIHR) via the Oxford Biomedical Research Centre.

References

1. Alonso AC, Grundke-Iqbal I, Iqbal K. Alzheimer's disease hyperphosphorylated tau sequesters normal tau into tangles of filaments and disassembles microtubules. Nat Med. 1996; 2:783–787. [PubMed: 8673924]
2. Arai T, Hasegawa M, Akiyama H, Ikeda K, Nonaka T, Mori H, Mann D, Tsuchiya K, Yoshida M, Hashizume Y, Oda T. TDP-43 is a component of ubiquitin-positive tau-negative inclusions in frontotemporal lobar degeneration and amyotrophic lateral sclerosis. Biochem Biophys Res Commun. 2006; 351:602–611. [PubMed: 17084815]
3. Arriagada PV, Growdon JH, Hedley-Whyte ET, Hyman BT. Neurofibrillary tangles but not senile plaques parallel duration and severity of Alzheimer's disease. J Neuropathol Exp Neurol. 1992; 42:631–639.
4. Balastik M, Lim JL, Pastorino L, Lu KP. Pin1 in Alzheimer's disease: multiple substrates, one regulatory mechanism? BBA-Mol Basis Dis. 2007; 1772:422–429.
5. Ball MJ. Topographic distribution of neurofibrillary tangles and granulovacuolar degeneration in hippocampal cortex of ageing and demented patients. A quantitative study. Acta Neuropathol. 1978; 42:73–80. [PubMed: 654888]

6. Bancher C, Brunner C, Lassmann H, Budka H, Jellinger K, Wiche G, Seitelberger F, Grundke-Iqbal I, Iqbal K, Wisniewski H. Accumulation of abnormally phosphorylated τ precedes the formation of neurofibrillary tangles in Alzheimer's disease. Brain Res. 1989; 477:90–99. [PubMed: 2495152]
7. Blom ES, Giedraitis V, Zetterberg H, Fukumoto H, Blennow K, Hyman BT, Irizarry MC, Wahlund LO, Lannfelt L, Ingelsson M. Rapid progression from mild cognitive impairment to Alzheimer's disease in subjects with elevated levels of tau in cerebrospinal fluid and the APOE epsilon4/epsilon4 genotype. Dement Geriatr Cogn Disord. 2009; 27:458–464. [PubMed: 19420940]
8. Bullock R. Future directions in the treatment of Alzheimer's disease. Expert Opin Investig Drugs. 2004; 13:303–314.
9. Braak H, Alafuzoff I, Arzberger T, Kretzschmar H, Del Tredici K. Staging of Alzheimer disease-associated neurofibrillary pathology using paraffin sections and immunocytochemistry. Acta Neuropathol. 2006; 112:389–404. [PubMed: 16906426]
10. Castellani RJ, Gupta Y, Siedlak SL, Harris PLR, Coller JM, Perry G, Zhu X, Tabaton M, Smith MA. Granulovacuolar degeneration in aging and Alzheimer's disease are the human homologue of stress granules precipitated by oxidative injury. 2010
11. Cleveland DW, Hwo SY, Kirschner MW. Purification of tau, a microtubule-associated protein that induces assembly of microtubules from purified tubulin. J Mol Biol. 1977; 116:207–225. [PubMed: 599557]
12. Davidson Y, Amin H, Kelley T, Shi J, Tian J, Kumaran R, Lashley T, Lees AJ, DuPlessis D, Neary D, Snowden JS, Sikkink S, Pickering-Brown SM, Mann DMA. TDP-43 in ubiquitinated inclusions in the inferior olives in frontotemporal lobar degeneration and in other neurodegenerative diseases: a degenerative process distinct from normal ageing. Acta Neuropathol. 2009; 118:359–369. [PubMed: 19330339]
13. Davidson Y, Kelley T, Mackenzie IRA, Pickering-Brown SM, Du Plessis D, Neary D, Snowden JS, Mann DMA. Ubiquitinated pathological lesions in frontotemporal lobar degeneration contain the TAR DNA-binding protein, TDP-43. Acta Neuropathol. 2007; 113:521–533. [PubMed: 17219193]
14. De Estable-Puig RF, De Estable-Puig JF. Vacuolar degeneration in neurons of aging rats. Virchows Arch B Cell Path. 1975; 17:337–346.
15. Dickson DW, Liu WK, Kress Y, Ku J, DeJesus O, Yen SH. Phosphorylated tau immunoreactivity of granulovacuolar bodies (GVB) of Alzheimer's disease: localization of two amino terminal tau epitopes in GVB. Acta Neuropathol. 1993; 85:463–470. [PubMed: 7684177]
16. Fagan AM, Mintun MA, Mach RH, Lee SY, Dence CS, Shah AR, LaRossa GN, Spinner ML, Klunk WE, Mathis CA. Inverse relation between in vivo amyloid imaging load and cerebrospinal fluid Aβ42 in humans. Ann Neurol. 2006; 59:512–519. [PubMed: 16372280]
17. Forsberg A, Engler H, Almkvist O, Blomquist G, Hagman G, Wall A, Ringheim A, Långström B, Nordberg A. PET imaging of amyloid deposition in patients with mild cognitive impairment. Neurobiol Aging. 2008; 29:1456–1465. [PubMed: 17499392]
18. Gendron TF, Petrucelli L. The role of tau in neurodegeneration. Mol Neurodegener. 2009; 4:13–29. [PubMed: 19284597]
19. Gotz J, Chen F, Barmettler R, Nitsch RM. Tau filament formation in transgenic mice expressing P301L tau. J Biol Chem. 2001; 276:529–534. [PubMed: 11013246]
20. Hashemzadeh-Bonehi L, Phillips RG, Cairns NJ, Mosaheb S, Thorpe JR. Pin1 protein associates with neuronal lipofuscin: potential consequences in age-related neurodegeneration. Exp Neurol. 2006; 199:328–338. [PubMed: 16480979]
21. Hendrie HC. Epidemiology of dementia and Alzheimer's disease. Amer J Geriatr Psychiatr. 1998; 6:19–21.
22. Hirano A, Dembitzer HM, Kurland LT, Zimmerman HM. The fine structure of some intraganglionic alterations. Neurofibrillary tangles, granular vacuolar bodies and 'rod-like' structures as seen in Guam amyotrophic lateral sclerosis and parkinsonism dementia complex. J Neuropathol Exp Neurol. 1968; 27:169–182.
23. Holzer M, Gärtner U, Stöbe A, Härtig W, Gruschka H, Brückner MK, Arendt T. Inverse association of Pin1 and tau accumulation in Alzheimer's disease hippocampus. Acta Neuropathol. 2002; 104:471–481. [PubMed: 12410395]

24. Khatoon S, Grundke-Iqbal I, Iqbal K. Brain levels of microtubule-associated protein tau are elevated in Alzheimer's disease: a radioimmuno-slot-blot assay for nanograms of the protein. J Neurochem. 1992; 59:750–753. [PubMed: 1629745]
25. Landau S, Harvey D, Madison C, Reiman E, Foster N, Aisen P, Petersen R, Shaw L, Trojanowski J, Jack C Jr, Weiner MW, Jagust WJ. Comparing predictors of conversion and decline in mild cognitive impairment. Neurology. 2010; 75:230–238. [PubMed: 20592257]
26. Lewis J, McGowan E, Rockwood J, Melrose H, Nacharaju P, Van Slegtenhorst M, Gwinn-Hardy K, Murphy MP, Baker M, Yu X. Neurofibrillary tangles, amyotrophy and progressive motor disturbance in mice expressing mutant (P301L) tau protein. Nat Genet. 2000; 25:402–405. [PubMed: 10932182]
27. Lim J, Ping Lu K. Pinning down phosphorylated tau and tauopathies. BBA-Mol Basis Dis. 2005; 1739:311–322.
28. Liou YC, Sun A, Ryo A, Zhou XZ, Yu ZX, Huang HK, Uchida T, Bronson R, Bing G, Li X. Role of the prolyl isomerase Pin1 in protecting against age-dependent neurodegeneration. Nature. 2003; 424:556–561. [PubMed: 12891359]
29. Lu KP, Zhou XZ. The prolyl isomerase PIN1: a pivotal new twist in phosphorylation signalling and disease. Nat Rev Mol Cell Biol. 2007; 8:904–916. [PubMed: 17878917]
30. Lu PJ, Wulf G, Zhou XZ, Davies P, Lu KP. The prolyl isomerase Pin1 restores the function of Alzheimer-associated phosphorylated tau protein. Nature. 1999; 399:784–788. [PubMed: 10391244]
31. Maddalena A, Papassotiropoulos A, Muller-Tillmanns B, Jung HH, Hegi T, Nitsch RM, Hock C. Biochemical diagnosis of Alzheimer disease by measuring the cerebrospinal fluid ratio of phosphorylated tau protein to {beta}-amyloid peptide42. Arch Neurol. 2003; 60:1202–1206. [PubMed: 12975284]
32. Mackenzie IRA, Neumann M, Bigio EH, Cairns NJ, Alafuzoff I, Kril J, Kovacs GG, Ghetti B, Halliday G, Holm IE, Ince PG, Kamphourst W, Revesz T, Rozemuller AJM, Kumar-Singh S, Akiyama H, Baborie A, Spins S, Dickson DW, Trojanowski JQ, Mann DMA. Nomenclature for neuropathologic subtypes of frontotemporal lobar degeneration: consensus recommendations. Acta Neuropathol. 2009; 117:15–18. [PubMed: 19015862]
33. Mackenzie IRA, Neumann M, Bigio EH, Cairns NJ, Alafuzoff I, Kril J, Kovacs GG, Ghetti B, Halliday G, Holm IE, Ince PG, Kamphourst W, Revesz T, Rozemuller AJM, Kumar-Singh S, Akiyama H, Baborie A, Spins S, Dickson DW, Trojanowski JQ, Mann DMA. Nomenclature for neuropathologic subtypes of frontotemporal lobar degeneration: an update. Acta Neuropathol. 2010; 119:1–4. [PubMed: 19924424]
34. Mann DM. Granulovacuolar degeneration in pyramidal cells of the hippocampus. Acta Neuropathol. 1978; 42:149–151. [PubMed: 654886]
35. McKhann GM, Albert MS, Grossman M, Miller B, Dickson D, Trojanowski JQ. Clinical and pathological diagnosis of frontotemporal dementia: report of the Work Group on Frontotemporal Dementia and Pick's Disease. Arch Neurol. 2001; 58:1803–1809. [PubMed: 11708987]
36. Neumann M, Sampathu DM, Kwong LK, Truax AC, Micsenyi MC, Chou TT, Bruce J, Schuck T, Grossman M, Clark CM. Ubiquitinated TDP-43 in frontotemporal lobar degeneration and amyotrophic lateral sclerosis. Science. 2006; 314:130–133. [PubMed: 17023659]
37. Neary D, Snowden JS, Gustafson L, Passant U, Stuss D, Black S, Freedman M, Kertesz A, Robert PH, Albert M. Frontotemporal lobar degeneration: a consensus on clinical diagnostic criteria. Neurology. 1998; 51:1546–1554. [PubMed: 9855500]
38. Piao YS, Wakabayashi K, Kakita A, Yamada M, Hayashi S, Morita T, Ikuta F, Oyanagi K, Takahashi H. Neuropathology with clinical correlations of sporadic amyotrophic lateral sclerosis: 102 autopsy cases examined between 1962 and 2000. Brain Pathol. 2003; 13:10–22. [PubMed: 12580541]
39. Price J, Davis P, Morris J, White D. The distribution of plaques, tangles and related immunohistochemical markers in healthy aging and Alzheimer's disease. Neurobiol Aging. 1991; 12:295–312. [PubMed: 1961359]

40. Ramakrishnan P, Dickson DW, Davies P. Pin1 colocalization with phosphorylated tau in Alzheimer's disease and other tauopathies. Neurobiol Dis. 2003; 14:251–264. [PubMed: 14572447]

41. Reynolds CH, Garwood CJ, Wray S, Price C, Kellie S, Perera T, Zvelebil M, Yang A, Sheppard PW, Varndell IM. Phosphorylation regulates tau interactions with Src homology 3 domains of phosphatidylinositol 3-kinase, phospholipase C gamma 1, Grb2, and Src family kinases. J Biol Chem. 2008; 283:18177–18186. [PubMed: 18467332]

42. Rocca W, Bonaiuto S, Lippi A, Luciani P, Turtu F, Cavarzeran F, Amaducci L. Prevalence of clinically diagnosed Alzheimer's disease and other dementing disorders: a door-to-door survey in Appignano, Macerata Province, Italy. Neurology. 1990; 40:626–631. [PubMed: 2320236]

43. Shi J, Shaw CL, Richardson AMT, Bailey K, Tian J, Varma AR, Neary D, Snowden JS, Mann DMA. Histopathological changes underlying frontotemporal lobar degeneration with clinicopathological correlation. Acta Neuropathol. 2005; 110:501–512. [PubMed: 16222525]

44. Tomlinson BE, Kitchener D. Granulovacuolar degeneration of hippocampal pyramidal cells. J Pathol. 1971; 106:165–185. [PubMed: 4114032]

45. Tapiola T, Alafuzoff I, Herukka SK, Parkkinen L, Hartikainen P, Soininen H, Pirttila T. Cerebrospinal fluid {beta}-amyloid 42 and tau proteins as biomarkers of Alzheimer-type pathologic changes in the brain. Arch Neurol. 2009; 66:382–389. [PubMed: 19273758]

46. Vincent I, Zheng JH, Dickson DW, Kress Y, Davies P. Mitotic phosphoepitopes precede paired helical filaments in Alzheimer's disease. Neurobiol Aging. 1998; 19:287–296. [PubMed: 9733160]

47. Wallin AK, Hansson O, Blennow K, Londos E, Minthon L. Can CSF biomarkers or pre-treatment progression rate predict response to cholinesterase inhibitor treatment in Alzheimer's disease? Int J Geriatr Psychiatry. 2009; 24:638–647. [PubMed: 19123199]

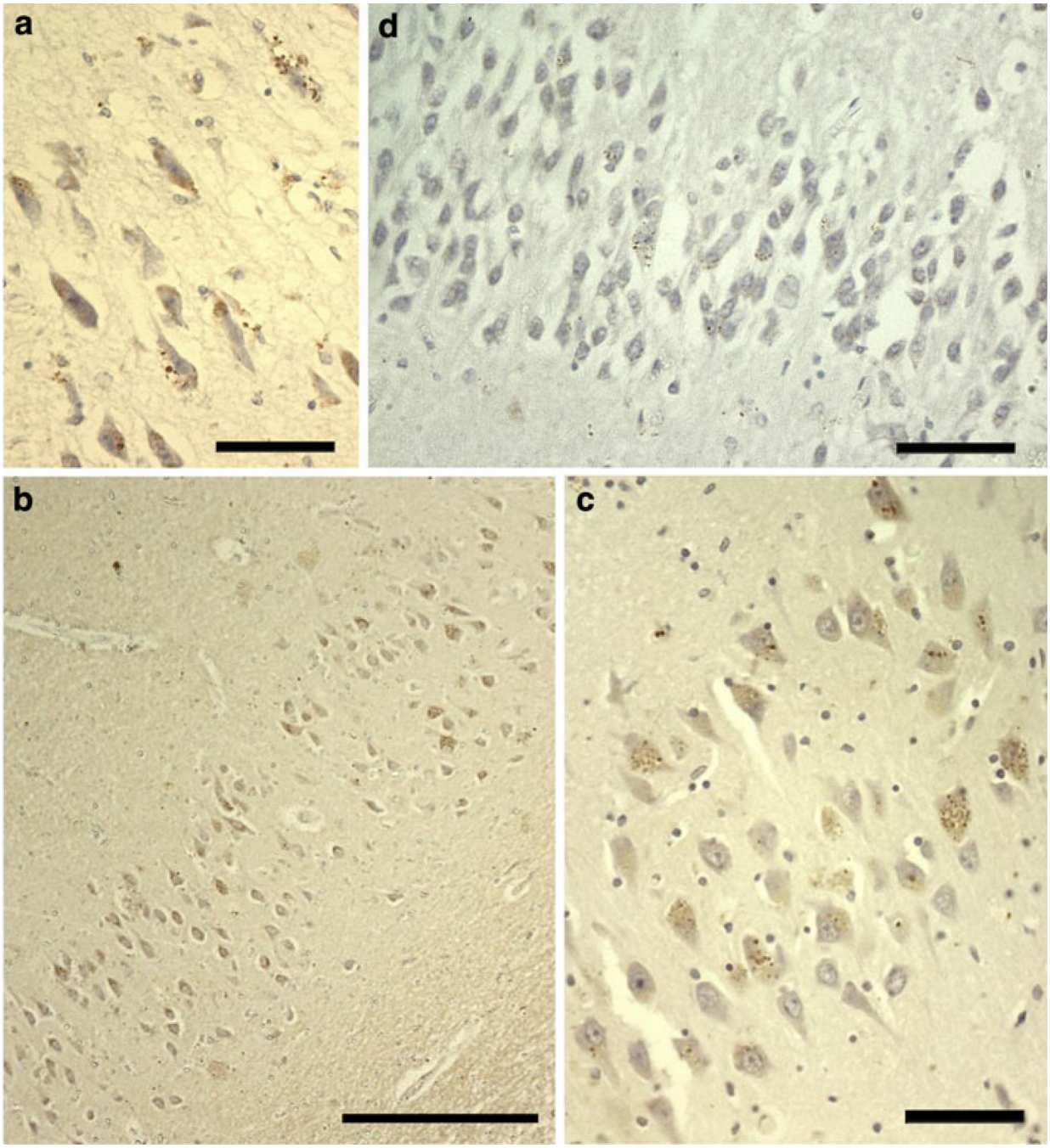

Fig. 1.

Morphological appearance of PIN1 granules in AD. Characteristic cytoplasmic granules contained within vacuoles are reminiscent of GVD (**a**). PIN1 granules occur more severely in CA1 (**b**) and CA2 (**c**), but also affect other regions such as the dentate gyrus (**d**). *Scale bars* **a, c, d** 20 μm, **b** 100 μm

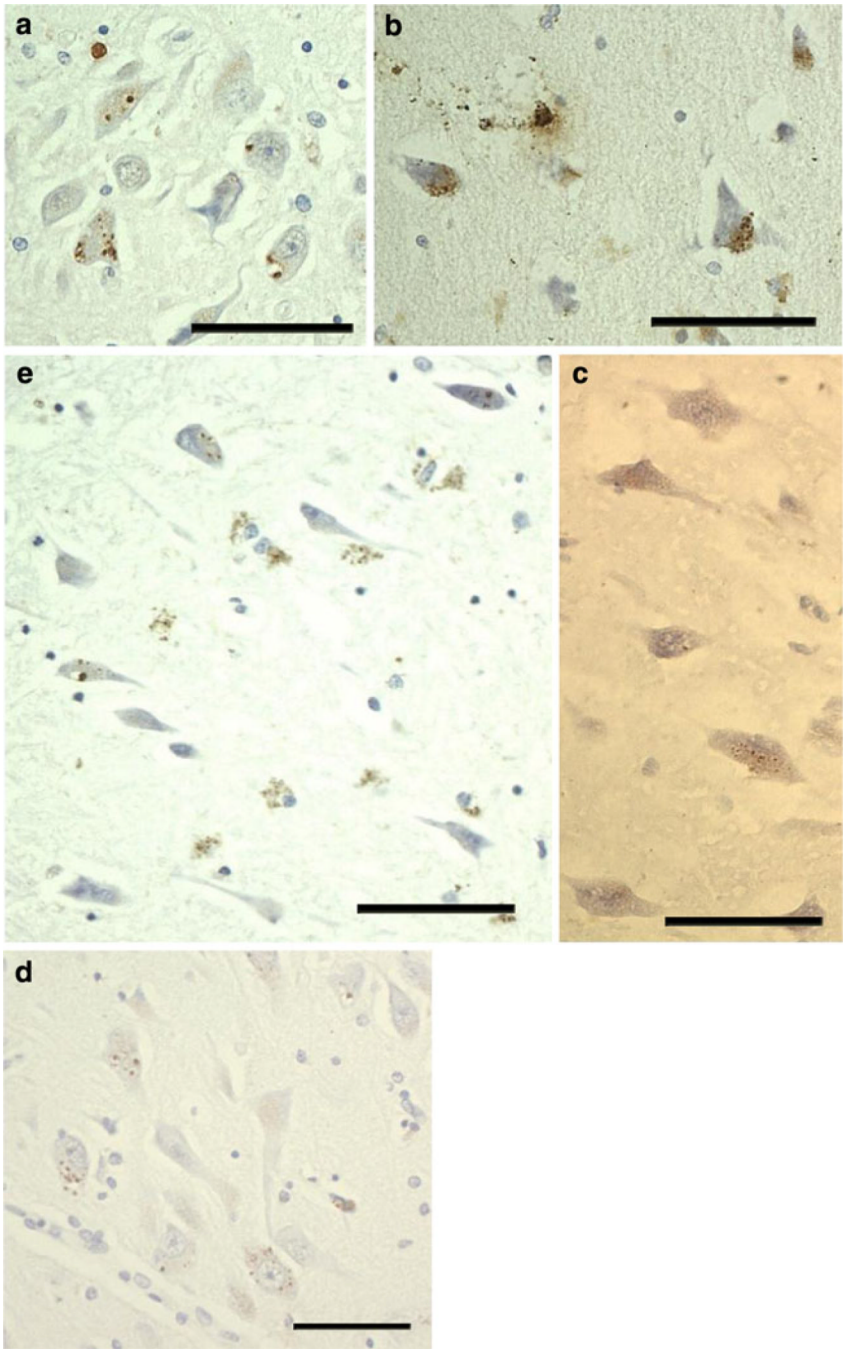

Fig. 2.

PIN1 granules in other disorders and in ND cases. The appearance of PIN1 granules is consistent in different groups and similar to those in **a** (**a–d**), except in FTLD cases where PIN1 granules show weaker immunoreactivity (**c**). There is preferential involvement of CA2 in PSP (**a**), FTLD (**c**) and PD (**d**). **b** PIN1 granules in CA4 in MND. **e** Involvement of CA1 in ND cases. All *scale bars* 20 μm

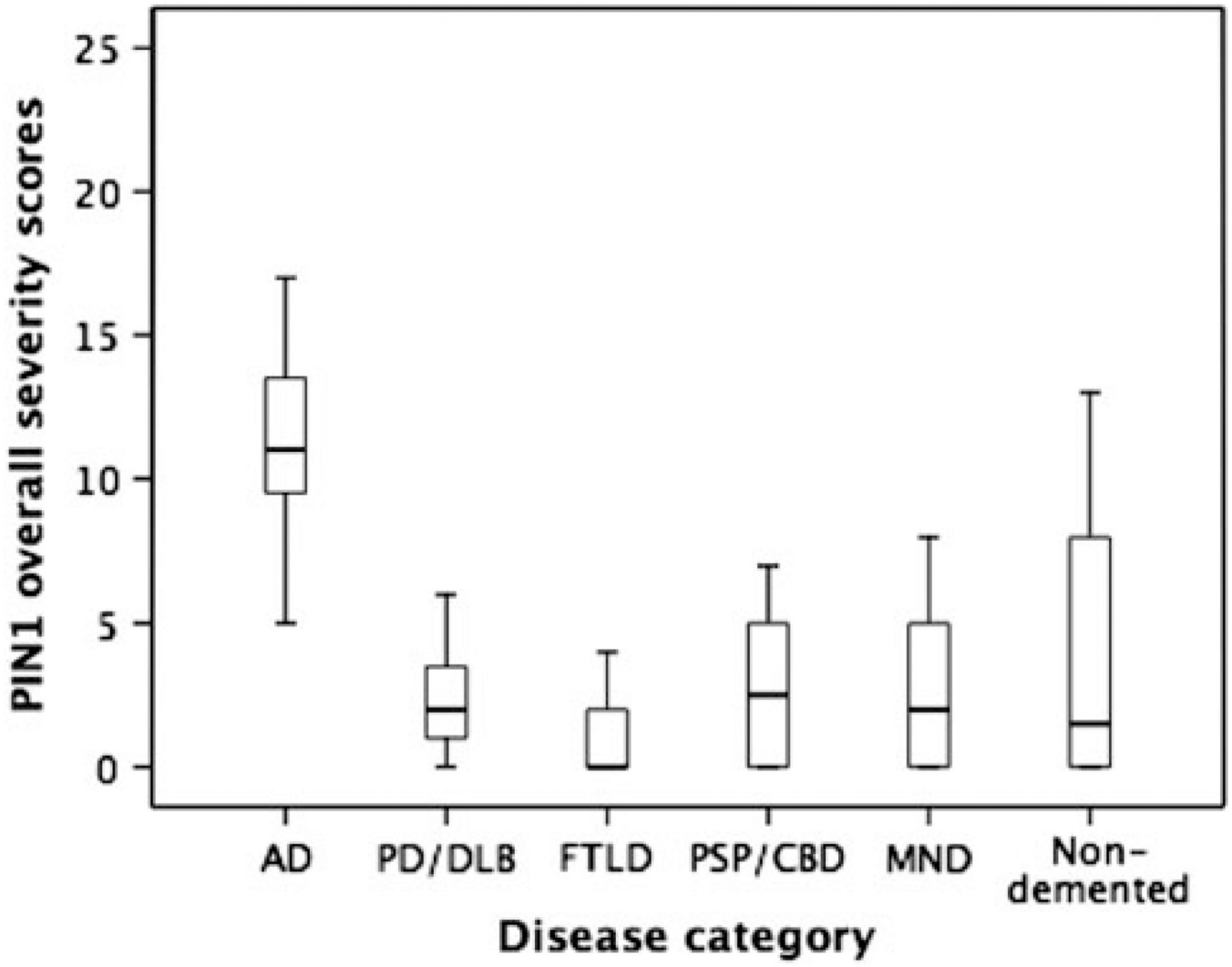

Fig. 3.
Box–whisker plots for the overall severity scores of PIN1 granules in the different diagnostic groups. The length of each *box* represents the interquartile range (75–25%) of the sample, the *solid line* drawn across the box the median and the *dashed line* the mean

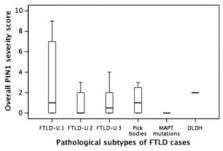

Fig. 4.

Box–whisker plots for the overall severity scores of PIN1 granules in the different FTLD subgroups. The length of each *box* represents the interquartile range (75–25%) of the sample, the *solid line* drawn across the box the median and the *dashed line* the mean

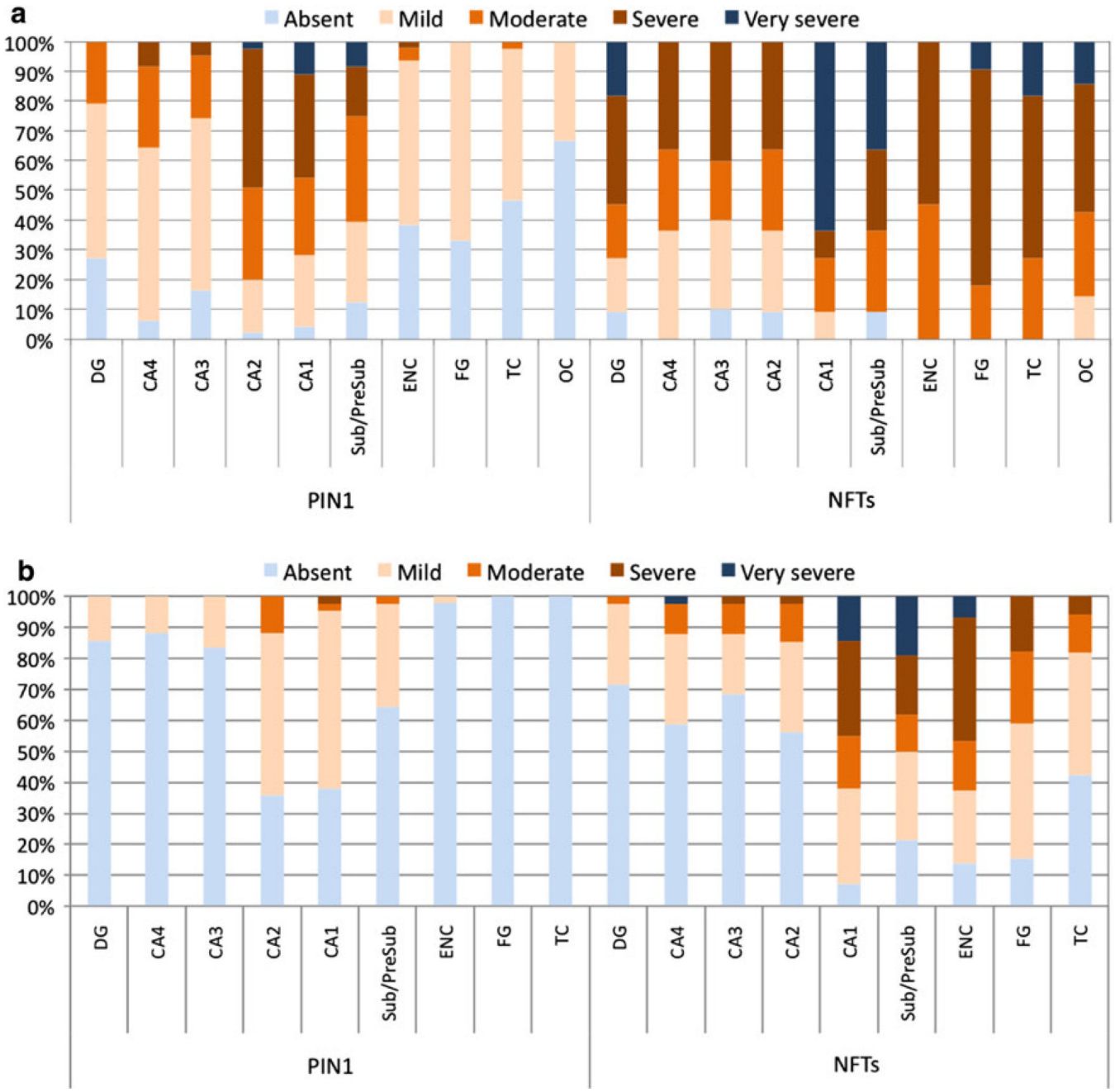

Fig. 5.

The distribution of PIN1 granules and NFTs in AD (**a**) and in PD/DLB (**b**). PIN1 granules occur more severely in CA1 and CA2 subfields and the subiculum in AD (**a**) but less so in cortical regions; a topographical pattern was also reflected in PD/DLB cases, though much less severely so (**b**). NFT distribution is independent of the distribution of PIN1 granules with NFT pathology occurring less severely in CA2 subfield and more frequently in cortical regions. Results are expressed as percentages of cases. *DG* dentate gyrus, *Sub/Presub* subiculum/presubiculum, *ENC* entorhinal cortex, *FG* fusiform gyrus, *TC* temporal cortex

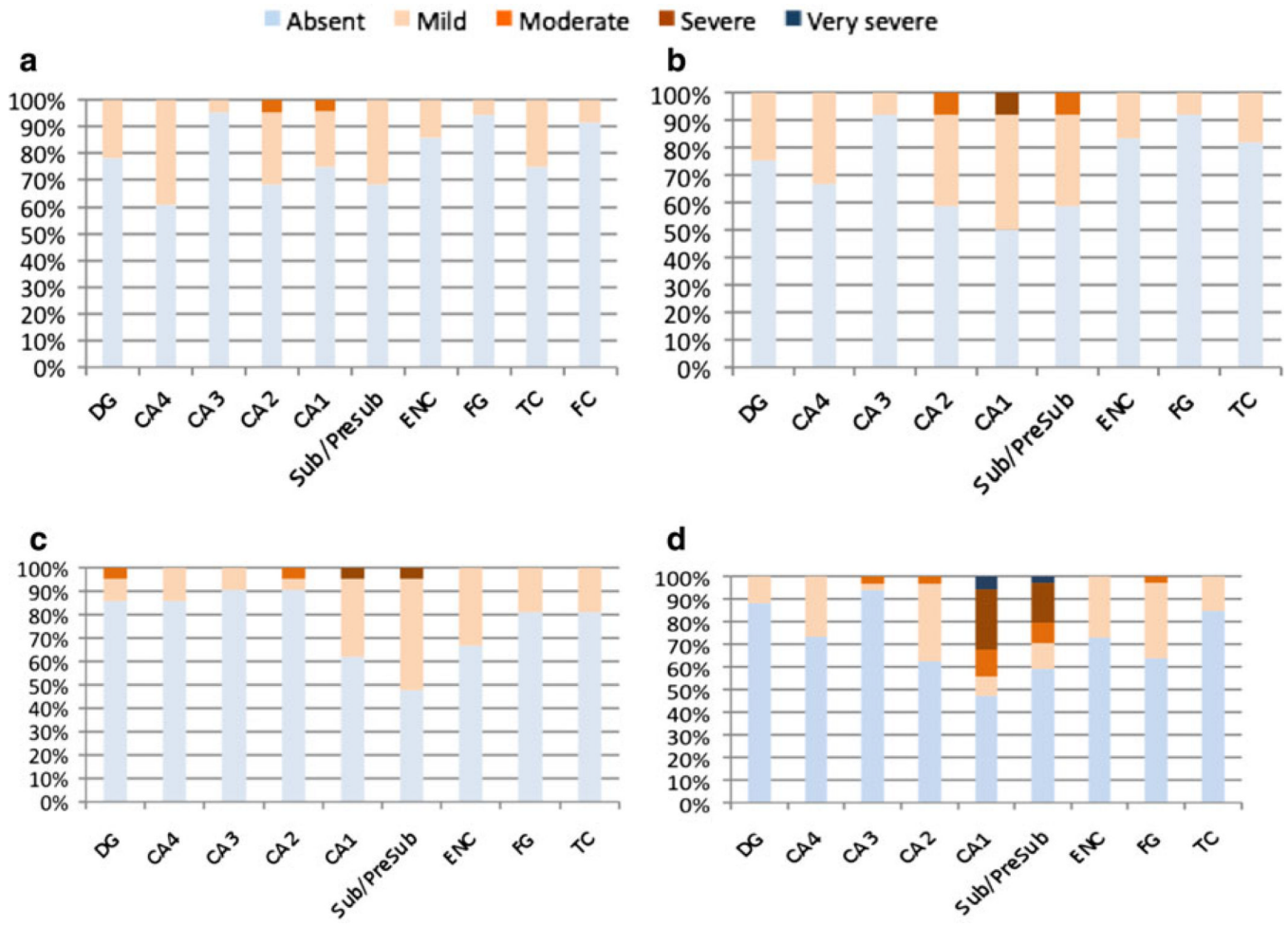

Fig. 6.

The distribution of PIN1 granules in FTLD (**a**), PSP/CBD (**b**), MND (**c**) and ND cases (**d**). Results are expressed as percentages of cases affected. *DG* dentate gyrus, *Sub/Presub* subiculum/presubiculum, *ENC* entorhinal cortex, *FG* fusiform gyrus, *TC* temporal cortex

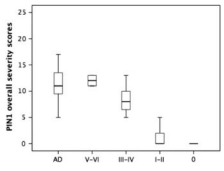

Fig. 7.

Box–whisker plots for overall severity scores of PIN1 granules in AD and ND cases, the latter being grouped according to Braak stages 0, I–II, III–IV and V–VI. The length of each *box* represents the interquartile range (75–25%) of the sample, the *solid line* drawn across the box the median and the *dashed line* the mean

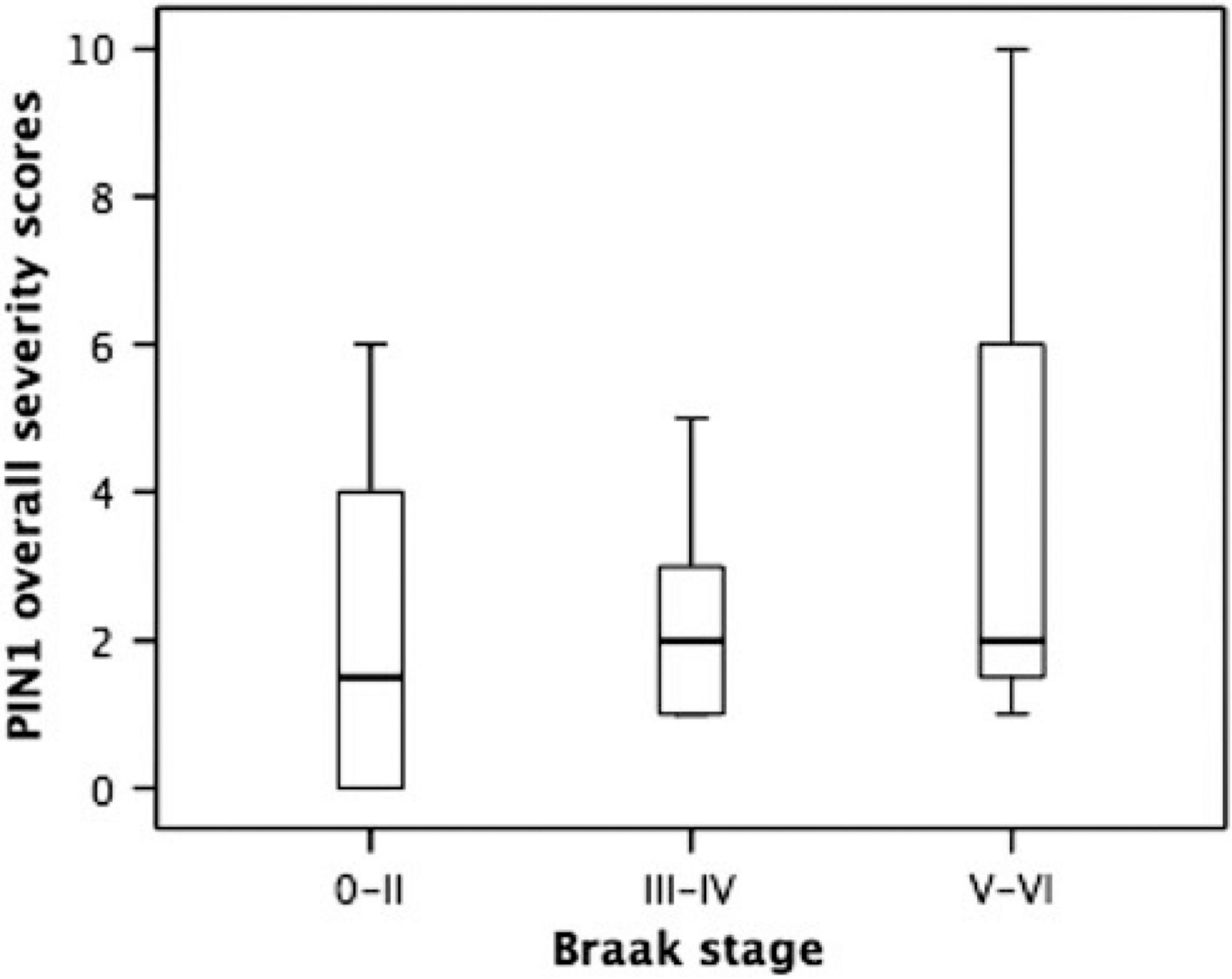

Fig. 8.

Box–whisker plots for overall severity scores of PIN1 granules in PD/DLB cases grouped according to Braak stages 0–II, III–IV and V–VI. The length of each *box* represents the interquartile range (75–25%) of the sample, the *solid line* drawn across the box the median and the *dashed line* the mean

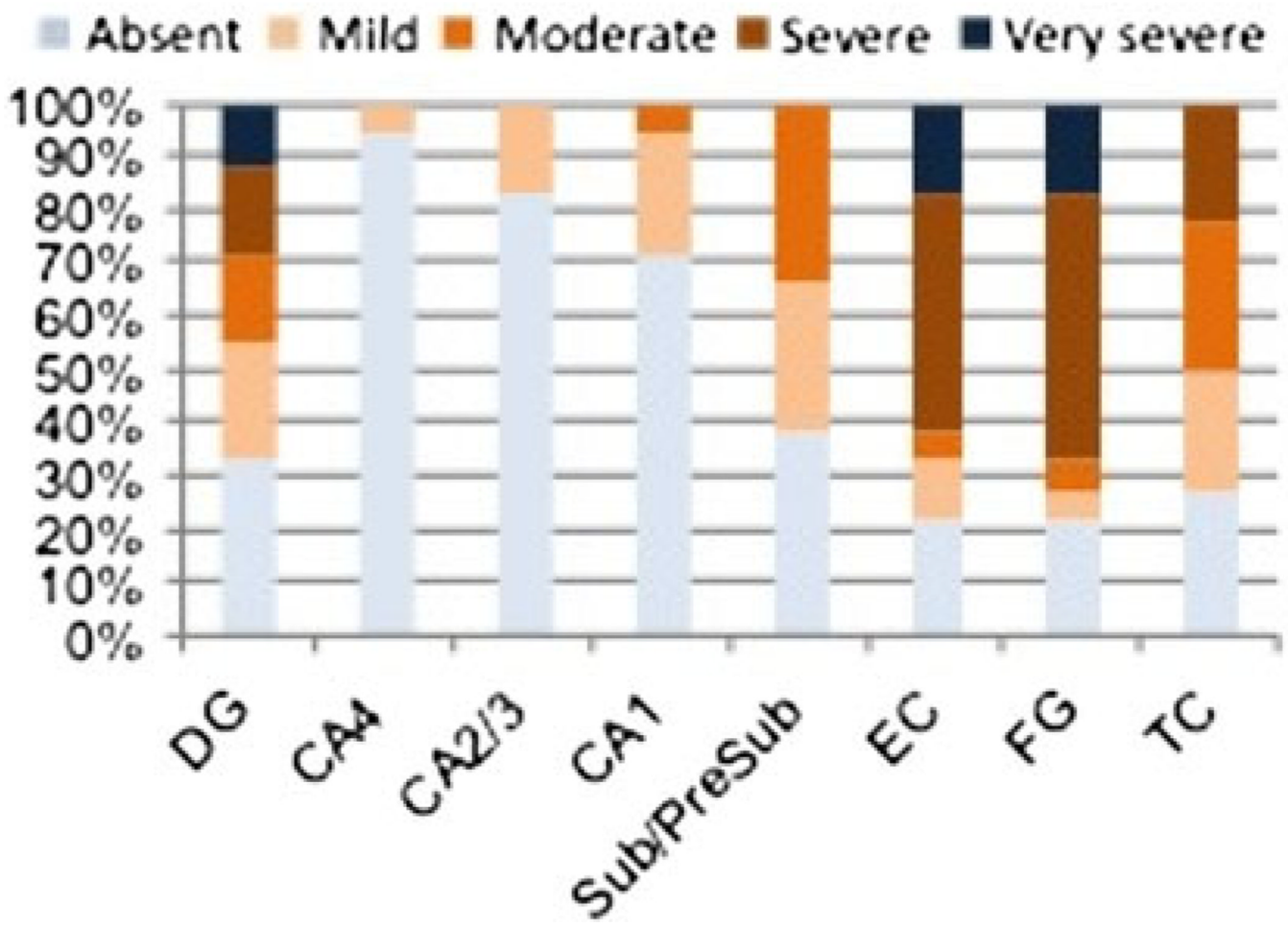

Fig. 9.
The distribution of TDP-43 pathological changes in AD. Results are expressed as percentages of cases affected. *DG* dentate gyrus, *Sub/Presub* subiculum/presubiculum, *ENC* entorhinal cortex, *FG* fusiform gyrus, *TCX* temporal cortex

Table 1

Demographic details of patients

	AD	PD/DLB	FTLD	PSP/CBD	MND	ND
Patients (*n*)	48	43	36	12	21	34
Age range (years)	50–92	54–89	31–80	64–91	45–72	26–94
Mean age ± SD (years)	71.7 ± 10.2	76.9 ± 7.7	63.9 ± 11.1	76.9 ± 10.6	61.7 ± 11.7	72.0 ± 20.1
Mean age at onset ± SD (years)	61.5 ± 11.4	63.9 ± 11.0	55.9 ± 11.6	69.3 ± 10.2	62.5 ± 3.5	–
Mean disease duration ± SD (years)	9.0 ± 3.5	13.2 ± 7.9	7.7 ± 4.5	7.7 ± 4.2	3.5 ± 2.1	–
Gender: male:female *N* (%)	17:26 (39.5:56.5)	32:9 (74.4:21.0)	21:12 (58.3:33.3)	10:2 (83:17)	13:7 (62:33)	11:21 (32.4:61.8)

AD Alzheimer's disease, *PD/DLB* Parkinson's disease/dementia with Lewy bodies, *FTLD* frontotemporal lobar degeneration, *PSP/CBD* progressive supranuclear palsy/corticobasal degeneration, *MND* motor neuron disease, *ND* non-demented

Acta Neuropathol. Author manuscript; available in PMC 2011 June 24.

Table 2

Proportion of cases affected by PIN1 granules in the different diagnostic groups

Diagnostic group	Present % (*n*)
AD (48)	100.0 (48)
PD/DLB (43)	79.1 (34)
FTLD (36)	44.4 (16)
PSP/CBD (12)	66.7 (8)
MND (21)	66.7 (14)
ND (34)	58.8 (20)

Table 3

Analysis showing the relationship between age at death and presence (+ve)/absence (−ve) of PIN1 immunoreactivity (PIN1-ir) or the overall severity scores of PIN1 granules

	Presence/absence of PIN1-ir*			PIN1 overall frequency rate per case	
	PIN1-ir +ve	PIN1-ir −ve	*P* value	Correlation coefficient	*P* value$^{\Psi}$
AD	71.7 ± 10.2	–	–	−0.07	0.660
PD/DLB	76.4 ± 8.1	79.3 ± 5.7	0.409	−0.03	0.850
PSP/CBD	80.4 ± 9.9	68.0 ± 6.1	0.030	0.19	0.002
FTLD	64.3 ± 12.9	63.4 ± 9.6	0.405	0.80	0.300
MND	61.7 ± 11.7	61.7 ± 11.7	–	0.01	0.980
ND	82.0 ± 6.3	57.7	0.003	0.58	<0.001

*P values calculated using either Student's t test or Mann–Whitney U test

$\Psi$$P$ values calculated using either Pearson's or Spearman's first rank correlations

Table 4

Correlations between the severity of PIN1 granules and NFTs in AD, PD/DLB and MND cases

	Correlation coefficient	*P* value
AD (*n* = 11)	0.590	0.056*
PD/DLB (*n* = 43)	0.276	0.073Ψ
MND (*n* = 12)	0.589	0.044*

*Pearson's correlation test

ΨSpearman's first rank correlation test

Table 5

Analysis of PIN1 mean overall severity scores in PD/DLB, FTLD, PSP/CBD and ND groups with (+ve) or without (−ve) amyloid-β (Aβ) plaque pathology

	N	Aβ +ve	Aβ −ve	*P* value*
PD/DLB	36	2.6 ± 3.4	2.2 ± 1.8	0.828
FTLD	36	3.3 ± 3.8	0.9 ± 1.2	0.115
PSP/CBD	12	3.8 ± 2.5	1.7 ± 2.1	0.131
ND	29	5.3 ± 4.8	0.7 ± 1.7	0.006

* *P* values calculated using either Student's *t* test or Mann–Whitney *U* test